Resonance of curved nanowires

L Calabri[1], N Pugno[2], W Ding[3] and R S Ruoff[3]

[1] CNR-INFM—National Research Center on nanoStructures and bioSystems at Surfaces (S3), Via Campi 213/a, 41100 Modena, Italy
[2] Department of Structural Engineering and Geotechnics, Politecnico di Torino, Turin, Italy
[3] Department of Mechanical Engineering, Northwestern University, Evanston, IL 60208-3111, USA

E-mail: calabri.lorenzo@unimore.it, nicola.pugno@polito.it, w-ding@northwestern.edu and r-ruoff@ northwestern.edu

Abstract
The effects of non-ideal experimental configuration on the mechanical resonance of boron (B) nanowires (NWs) were studied to obtain the corrected value for the Young's modulus. The following effects have been theoretically considered: (i) the presence of intrinsic curvature, (ii) non-ideal clamps, (iii) spurious masses, (iv) coating layer, and (v) large displacements. An energy-based analytical analysis was developed to treat such effects and their interactions. Here, we focus on treating the effect of the intrinsic curvature on the mechanical resonance. The analytical approach has been confirmed by numerical FEM analysis. A parallax method was used to obtain the three-dimensional geometry of the NW.

(Some figures in this article are in colour only in the electronic version)

1. Introduction

Uniaxial nanostructures such as nanotubes, nanowires, nanorods and nanowhiskers are of recent interest. Two commonly used methods to study the mechanical properties of uniaxial nanostructures are the mechanical resonance method and the tensile testing method (Ding *et al* 2006). The resonance method has been frequently used to probe the stiffness of nanostructures (Poncharal *et al* 1999, Wang *et al* 2000a, 2000b, Bai *et al* 2003, Dikin *et al* 2003, Calabri 2005). As reported in this paper, there are many factors that may affect the results in terms of the fit value and spread of values of Young's modulus.

In this work we focus, in particular, on treating the effect of the intrinsic curvature on the mechanical resonance of the beam-shaped structures, analysing experimental data (Ding *et al* 2006) of curved boron (B) nanowires (NWs).
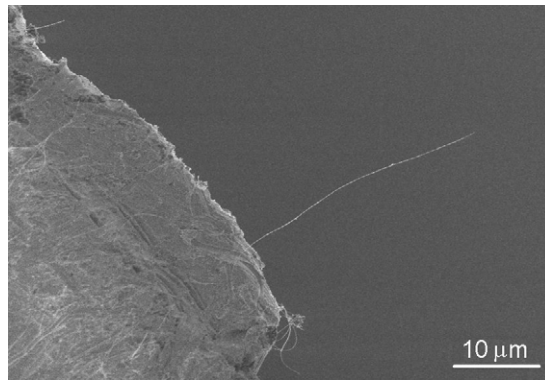
Figure 1. SEM image of CVD-grown crystalline B NWs projecting from the edge of a TEM grid.

Mechanical resonance can be induced when the frequency of the applied force (the forcing frequency) approaches the nth normal mode frequency of the NW. According to the *simple beam theory*, the nth mode resonance frequency f_n of a clamped–free uniform beam, is given by

$$f_n = \frac{\beta_n^2}{2\pi} \sqrt{\frac{E_0 I}{m L^4}} \tag{1}$$

where E_0 is the Young's modulus of the beam, I is the cross-section moment of inertia, m is the mass per unit length, and L is the beam length. The term β_n is a constant value depending on the resonance mode ($\beta_0 = 1.875$, $\beta_1 = 4.694$, $\beta_2 = 7.855$ and $\beta_3 = 10.996$: values of β_n for the first four resonance modes).

Mechanical resonance measurements were performed on chemical vapour deposition (CVD)-grown crystalline B NWs (Otten *et al* 2002), and the Young's modulus values for each were calculated according to the beam theory (Ding *et al* 2006). To apply the classical beam theory, several hypotheses have to be verified (Meirovich 1975). The experimental conditions often disagree with the hypotheses introduced with the elastic theory; for this reason we tried to consider effects such as the driving condition (excitation), NW curvature, boundary conditions and different kind of surface irregularities (presence of spurious masses and/or deposition of a layer of material during the experiment), with an energy-based analytical analysis based on the Rayleigh–Ritz method.

2. Experimental configuration

The crystalline B NWs used were previously synthesized by a catalysed chemical vapour deposition method (Otten *et al* 2002; we appreciate receiving the sample used from Otten). They are tens of microns in length with diameters in the range 20–200 nm. Figure 1 shows an SEM image of such B NWs projecting from the edge of a TEM grid.

The whole resonance measurement was performed (Ding *et al* 2006) inside an SEM chamber. The B NWs tested were first clamped to the tip of an AFM cantilever using the EBID process (Ding *et al* 2005) (figures 3(a) and (b)), and then removed from the source using a home-built nano-manipulator (Yu *et al* 1999). The AFM cantilever, with the NW clamped on its tip, is connected to the stage of the nano-manipulator through a piezo-bimorph actuator (figures 2(a) and (b)). During the resonance measurement, a clamped–free NW was excited
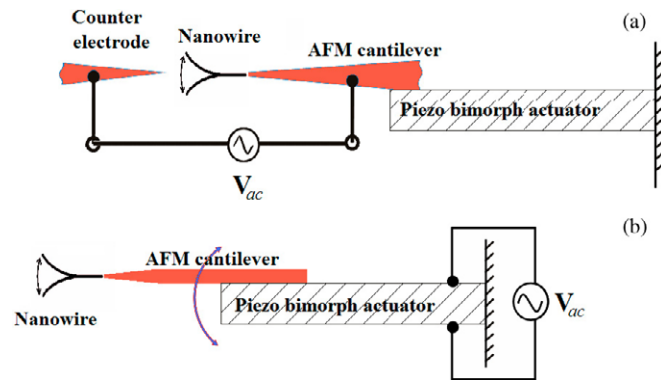
Figure 2. (a) Electrical excitation of a cantilevered boron nanowire. (b) Mechanical excitation of a cantilevered boron nanowire.
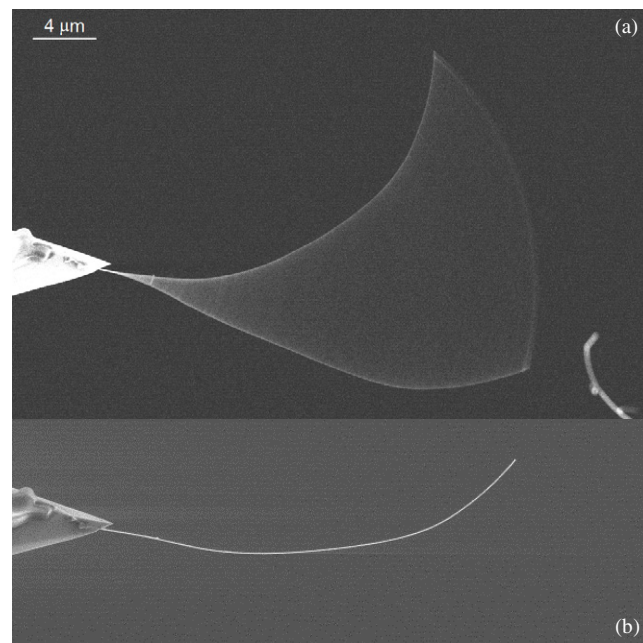

Figure 3. (a) Resonance of the first mode of vibration of the curved B NW shown in (b), attached to an AFM tip.

to resonance by applying a mechanically or electrically induced periodic force to it. In the electrical excitation method (figure 2(a)), an ac voltage with tunable frequency was applied between the AFM cantilever and the counter electrode, thus an alternating electric field is created in the area around the B NW. In the mechanical excitation method (figure 2(b)), the ac voltage was directly applied to a piezo-bender to induce the mechanical vibration of the cantilever and consequently of the NW attached to it. Either way, the resonance of the B NW can be excited as the ac signal frequency matches its proper frequency.

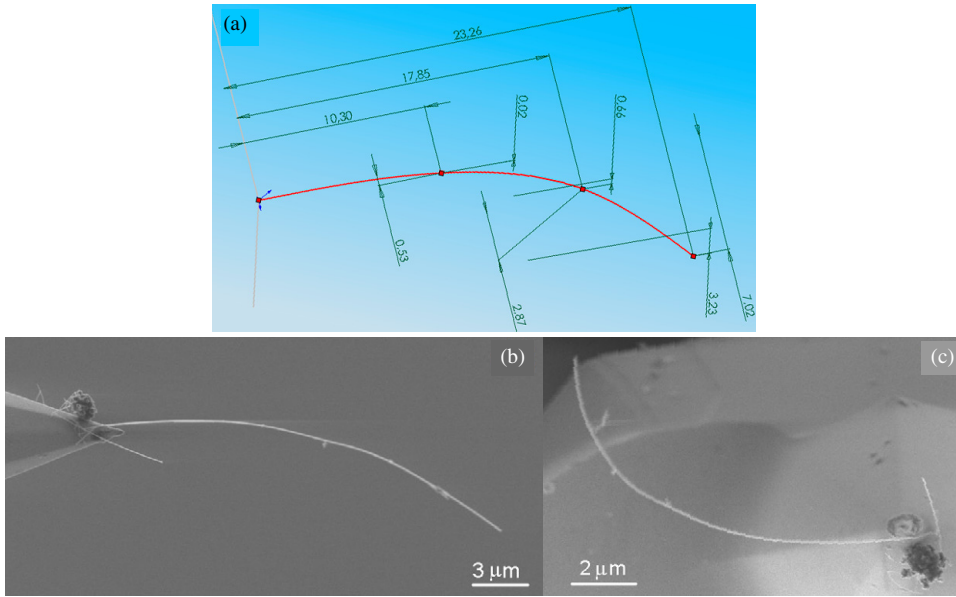For other experimental details please refer to Ding *et al* (2006).

Figure 4. (a) 3D reconstruction of a real B NW ((b), (c)) modelled with CAD software. The units of measurements reported in (a) are μm. The SEM images ((b), (c)) refer to the same wire and are obtained by tilting the sample with a 90° angle. They are necessary to apply the parallax method (Huang *et al* 2004) and to reconstruct the 3D configuration.

3. Results and discussion

3.1. Resonance measurement results

During experiments (Ding *et al* 2006) the resonance frequency of several B NWs tested was recorded. Figure 3 shows SEM images of the first mode resonance of a cantilevered B NW attached to an AFM tip.

Since SEM images only gave a two-dimensional (2D) projection of the NW, there could be some errors in the length measurement if the NW is not parallel to the plane of projection. As shown in equation (1), the Young's modulus is proportional to the fourth power of the beam length. Young's modulus is thus particularly sensitive to errors in the length. To accurately measure the NW length, a parallax method was used to reconstruct the three-dimensional (3D) configuration of the nanowire (Huang *et al* 2004). Figure 4(a) shows the 3D reconstruction of a real B NW (figures 4(b) and (c)) obtained with CAD software (SolidWorks® 2005, SolidWorks Corporation). These measurements are to determine the spatial coordinates of the reference points representing the characteristic of the beam curvature.

With accurate NW geometry (L, I and m) and resonance frequency data (f_n), the Young's moduli of the NWs were calculated according to equation (1), converted in order to express the Young's modulus directly:

$$E_0 = \frac{4\pi^2 m L^4}{\beta_n^4 I} f_n. \tag{2}$$

The measured Young's moduli of the curved B NWs ranged between 150 and 250 GPa, as listed in table 1. (As discussed in detail in our previous work (Ding *et al* 2006), there is an amorphous oxide layer covering the NWs. Here we did not make corrections to take into
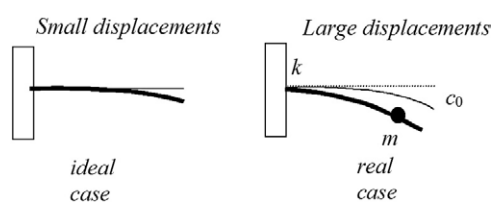
Figure 5. In the ideal case the clamp is infinitely rigid and the NW is perfectly straight, with no spurious masses attached on it and no coating deposited on its surface. In the real case these four effects often co-exist and thus would be interacting. In addition, the role of the finite kinematics (large displacements) could be significant.

Table 1. The Young's modulus of curved B NWs.

Sample #	Length[a] (μm)	Diameter[b] (nm)	Frequency[b] (kHz)	Young's modulus[c] (GPa)
11-06 #1	16.2 ± 0.2	75 ± 1	346 ± 0.05	218 ± 18
11-29 #2	7.8 ± 0.2	70 ± 1	1295 ± 0.05	155 ± 17
12-09 #2	22.2 ± 0.2	103 ± 2	440 ± 0.05	362 ± 11
12-22 #1	25.6 ± 0.4	78 ± 2	106 ± 0.05	96 ± 11
01-10 #1	7.8 ± 0.2	64 ± 3	1332 ± 0.05	196 ± 42

[a] Wire length: obtained with the parallax method based on the experimental data (see note b).
[b] Wire geometry and frequency: results obtained from experiment (Ding *et al* 2006).
[c] Fit values are expected to be affected by the non-ideal configuration of the experimental set-up.

account the boron oxide layer, so the Young's modulus listed is the average value of an oxide-coated B NW and not the Young's modulus of the B core. Please refer to Ding *et al* (2006) for a detailed analysis considering the boron oxide layer.) The main point of our treatment of the influence of curvature is of its influence on the resonance frequency of a cantilevered beam. The fact that we have a core–shell structure versus a structure homogeneous throughout is thus a secondary issue for the analysis presented below.

The results reported in table 1 are obtained using the simple beam theory, considering the NWs tested as ideal beams (straight, uniform and rigidly clamped); nevertheless to apply this theory there are several assumptions that are rendered not completely valid, by the non-ideal configuration.

The three-dimensional reconstruction of the NW is very important also for the *correction procedure* (see section 3.2 below) and for the FEM simulation (section 3.3), where the exact geometry of the NWs (length and curvature radius) is necessary to rationalize the experimental results.

3.2. Correction procedure

The Young's modulus values of these curved NWs listed in table 1 are much lower than the modulus of bulk crystalline boron (Tavadze *et al* 1981). Several factors were believed to contribute to this issue (figure 5): (i) foremost, the amorphous coating layer, (ii) intrinsic curvature of the wire, (iii) non-ideal boundary conditions, (iv) the possible presence of spurious attached particles, and (v) large displacements. We neglected the effect of the possible presence of nanocracks in the NWs (Pugno *et al* 2000, Carpinteri and Pugno 2005a, 2005b).

We tried to consider all these factors with an analytical approach based on the classical Rayleigh–Ritz method. We carried out an expression available for the Young's modulus of a non-ideal wire (neglecting the effects related to the second order corrections due to the

interaction between the causes):

$$E \approx E_0(1 + c_r C_r + c_\delta C_\delta + c_c C_c - c_k C_k - c_q C_q) \tag{3}$$

where E_0 is the Young's modulus derived neglecting the effects (i), (ii), (iii), (iv) and (v); C_r, C_δ, C_c, C_k and C_q are the coefficients which take account of the non-ideal boundary conditions (C_k), intrinsic curvature of the wire (C_r), spurious masses (C_q), large displacements (C_δ) and amorphous coating layer (C_c); and c_r, c_δ, c_c, c_k, and c_q are positive constants.

In particular:

$$C_k = \frac{E_0 I}{kL}; \quad C_r = \frac{L^2}{r^2}; \quad C_q = \frac{q}{mL}\alpha^4; \quad C_\delta = \frac{\delta^2}{L^2}; \quad C_c = \frac{t}{R}\beta \tag{4}$$

$$\alpha = \frac{z}{L} \quad \text{and} \quad \beta = 1 + \frac{\rho_c}{\rho} - 2\frac{E_c}{E_0} \tag{5}$$

where k is the rotational stiffness of the clamp; r is the intrinsic curvature radius; q is the spurious particle mass; δ is the amplitude of the tip oscillations; ρ_c is the density and E_c is the Young's modulus of the coating layer (shell) with thickness t enveloping the B core having radius R, density ρ and Young's modulus E_0; α represents the mass particle position on the wire with reference to the edge of the clamp and β is a factor which takes into account the density and the Young's modulus of the coating layer.

The formula (3) is particularly easy to apply and takes into account each 'problem' linked with the non-ideal configuration of the experimental set-up, to first order in each. The multiplying factors (c_k, c_r, c_q, c_δ, c_c) have to be 'calibrated' with a numerical procedure in order to obtain a generic formula available for a wide range of tested beams.

In this paper we present only the determination of the intrinsic curvature multiplying factor c_r (section 3.3), considering only the problems linked with the curvature of the B NWs. It remains to consider the other non-ideal effects and to calibrate the other factors so as to obtain a complete formula.

3.3. Vibration of curved nanowire

The five NWs listed in table 1 are all curved NWs. Since the equation (1) we used to calculate the Young's modulus is for a straight cantilevered beam (simple beam theory hypothesis), applying this formula to a curved structure introduces errors. To obtain the true Young's modulus of the curved NWs and to calibrate the correction factor in formula (3), we carried out FEM simulations with ANSYS® software (Ansys 8.0, Ansys Inc.) by running a modal analysis.

First an ideal straight NW was modelled (figure 6) to ensure that the numerical results were correct and the simple beam theory verified. In this way we checked the quality of the FEM model used. Then the same modelling procedure was applied to those B NWs with a curved geometry (figure 7), giving a correction comparable to that deduced by equation (6) (table 2).

As discussed before, we used a parallax method to reconstruct the 3D configuration of the NWs (Huang *et al* 2004). Using this method, the spatial coordinates of several reference points, representing the characteristic of the beam curvature (figure 4(a)), were exported to ANSYS®, and a spline was designed with the same shape as the curved nanowire. Then an FEM was created by extruding the NW cross-section area along the spline. Attention was paid to ensuring the symmetry of the structure because a small error in the symmetry of the beam can significantly affect the resonance frequency of the structure as obtained by the modal analysis. The clamped–free configuration was used in the modelling, thus directly relevant to the boundary condition present in the experiment.
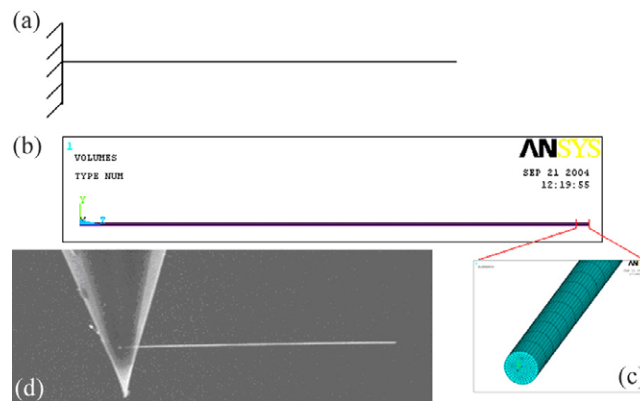
Figure 6. ANSYS model of a straight B NW. (a) Schematic diagram of a cantilevered straight B NW. (b) FEM model of the B NW (the inset (c) shows a section of the model, so one can see the radial distribution of the elements in the section). (d) SEM image of the cantilevered straight B NW modelled.
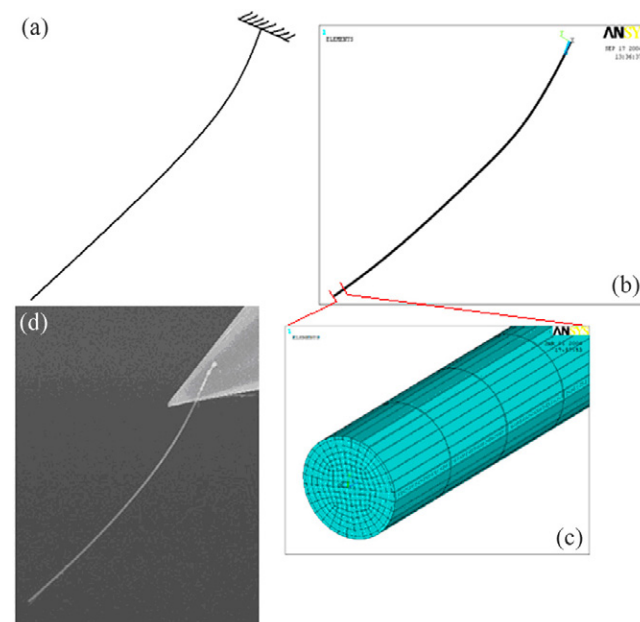

Figure 7. ANSYS model of a curved B NW. (a) Schematic diagram of a cantilevered curved B NW. (b) FEM model of the B NW (the inset (c) shows a section of the model, so one can see the radial distribution of the elements in the section). (d) SEM image of the cantilevered curved B NW modelled.

The Young's modulus values of each of the B NWs modelled were obtained from the simulation using the measured frequency values.

Table 2 shows the numerical simulation results for Young's modulus for the five curved B NWs treated. These results are compared in the table with the values of the Young's modulus of the corresponding straight NW of same length and with the values corrected with the theoretical procedure. As mentioned, we considered only the effect of the curvature both

Table 2. Comparison between the Young's modulus of the curved NWs corrected with theoretical and numerical (FEM) models.

Sample #	Length (μm)	Diameter (nm)	Frequency (kHz)	Modulus assumed straight (GPa)	Modulus corrected (Theo) (GPa)	Modulus corrected (Num) (GPa)
11-06 #1	16.2	75	346	218	207.7	204.9
11-29 #2	7.8	70	1295	155	151.6	152
12-09 #2	22.2	103	440	362	356.5	356
12-22 #1	25.6	78	106	96	91.9	91.9
01-10 #1	7.8	64	1332	196	194.5	194.2

in the theoretical model than in the FEM one. There is good agreement between the numerical and theoretical results, which suggests that this method allows straightforward evaluation of the Young's modulus of curved NWs.

The constant c_r for the intrinsic curvature was obtained from the numerical simulation results. We find that c_r is equal to 1/25, thus one has

$$E_{\text{curve}} \approx E_{\text{straight}}\left(1 + \frac{L^2}{25r^2}\right). \tag{6}$$

We used this formula to evaluate the 'corrected' Young's modulus for the curved NWs analysed from experimental data (table 2). All the samples reported in table 1 have a curved shape; thus we applied the formula (6) for these. The numerical and theoretical approaches clearly yield similar values.

As mentioned above, our goal here is not to treat the modulus of the B core, but instead to develop a method to account for the influence of curvature on the fit value of the modulus of the curved NW.

4. Concluding remarks

In this paper we investigated the effects of non-ideal experimental configuration and found a straightforward method to correct the simple beam theory when its fundamental hypotheses are not strictly verified, particularly with respect to curved versus straight beams. We used an energy technique based on the classical Rayleigh–Ritz method, yielding formula (6). We developed a numerical FEM analysis to consider the effect of the beam curvature on the value of the Young's modulus of the samples treated and furthermore to 'calibrate' a constant in the formula in order to confirm the efficiency of this analytical approach. The nanowire diameter and length were carefully determined, and a 3D reconstruction method was used to get the true wire length. This is necessary both to use the simple beam theory and to model the real shape of the wire in an FEM software.

Here, we focused on treating the effect of the intrinsic curvature on the mechanical resonance, obtaining a good agreement between the numerical and theoretical results (as reported in table 2). The future directions include extending this method of achieving a 'calibration' of the other 'correction' coefficients so as to obtain a complete analytical procedure for the vibration of real nanowires. In fact the non-ideal effects, such as (i) intrinsic curvature of the wire, (ii) non-ideal boundary conditions, (iii) amorphous coating layer, (iv) spurious attached particle, and (v) large displacements, are often present on real NWs and they all affect the proper resonance frequency of the sample depending on the level of the non-ideality (as one can deduce from equations (3) and (4)). We decided first to focus on the intrinsic curvature of the nanowire because it often affects the shape of the B NWs, changing in a significant way the value of their mechanical properties.

Acknowledgments

References

Bai X D, Gao P X, Wang Z L and Wang E G 2003 Dual-mode mechanical resonance of individual ZnO nanobelts *Appl. Phys. Lett.* **82** 4806–8

Calabri L 2005 Materiali nanostrutturati—NanoCompositi e NanoRivestimenti *PhD Thesis* (6 of 36 months were with the Ruoff Group, Northwestern University, Evanston, IL, USA) Dipartimento di Meccanica e Tecnologie Industriali (DMTI), Università degli Studi di Firenze. Firenze, Italy

Carpinteri A and Pugno N 2005a Towards chaos in vibrating damaged structures—part I. Theory and period doubling cascade *J. Appl. Mech.* **72** 511–8

Carpinteri A and Pugno N 2005b Towards chaos in vibrating damaged structures—part II. Parametrical investigation *J. Appl. Mech.* **72** 519–26

Dikin D A, Chen X, Ding W, Wagner G and Ruoff R S 2003 Resonance vibration of amorphous SiO_2 nanowires driven by mechanical or electrical field excitation *J. Appl. Phys.* **93** 226–30

Ding W, Calabri L, Chen X, Kohlhaas K M and Ruoff R S 2006 Mechanics of crystalline boron nanowires *Compos. Sci. Technol.* **66** 1112–24

Ding W, Dikin D A, Chen X, Piner R D, Ruoff R S, Zussman E, Wang X and Li X 2005 Mechanics of hydrogenated amorphous carbon deposits from electron-beam-induced deposition of a paraffin precursor *J. Appl. Phys.* **98** 014905

Huang Z, Dikin D A, Ding W, Qiao Y, Chen X, Fridman Y and Ruoff R S 2004 Three-dimensional representation of curved nanowires *J. Microsc.* **216** 206–14

Meirovich L 1975 *Elements of Vibration Analysis* (New York: McGraw-Hill) p 495

Otten C J, Lourie O R, Yu M-F, Cowley J M, Dyer M J, Ruoff R S and Buhro W E 2002 Crystalline boron nanowires *J. Am. Chem. Soc.* **124** 4564–5

Poncharal P, Wang Z L, Ugarte D and de Heer W A 1999 Electrostatic deflections and electromechanical resonances of carbon nanotubes *Science* **283** 1513–6

Pugno N, Ruotolo R and Surace C 2000 Evaluation of the non-linear dynamic response to harmonic excitation of a beam with several breathing cracks *Int. J. Sound Vib.* **235** 749–62

Tavadze F N, Lominadze J V, Khvedelidze A G, Tsagareishvili G V, Shorshorov M K and Bulichev S I 1981 The effect of impurities on the mechanical-properties of zone-melted boron *J. Less-Common Met.* **82** 95–9

Wang Z L, Dai Z R, Gao R P, Bai Z G and Gole J L 2000a Side-by-side silicon carbide–silica biaxial nanowires: synthesis, structure, and mechanical properties *Appl. Phys. Lett.* **77** 3349–51

Wang Z L, Poncharal P and de Heer W A 2000b Nanomeasurements of individual carbon nanotubes by *in situ* TEM *Pure Appl. Chem.* **72** 209–19

Yu M F, Dyer M J, Skidmore G D, Rohrs H W, Lu X K, Ausman K D, Von Ehr J R and Ruoff R S 1999 Three-dimensional manipulation of carbon nanotubes under a scanning electron microscope *Nanotechnology* **10** 244–52